High-Resolution Time-of-Flight Mass Spectra of Alkanethiolate-Coated Gold Nanocrystals

Randy J. Arnold and James P. Reilly*

Contribution from the Department of Chemistry, Indiana University, Bloomington, Indiana 47405

Received July 14, 1997

Abstract: Alkanethiolate-coated gold nanocrystals have been laser desorbed from a solid film, ionized, and analyzed by time-of-flight mass spectrometry. A previously unresolved distribution of peaks is observed and the number of gold and sulfur atoms associated with each feature can be assigned. Alkyl chains are not evident in these high-resolution spectra. Experiments using spatially and temporally separated light pulses demonstrate that more of the desorbed nanocrystals are neutral than are ionized. Pure gold cluster ions of various sizes can be generated from these neutral molecules in the two-laser experiment.

Alkanethiolate-coated gold nanocrystals consist of a central core of 10s to 1000s of gold atoms that is surrounded by an adsorbed alkanethiolate monolayer.[1] The organic molecules are believed to self-assemble onto the core in a manner similar to their binding to bulk gold. The unique size and composition of these particles lead to a number of unusual physical, electronic, and chemical properties that have motivated their study.[2] "Coulomb staircase" behavior and electron hopping have been observed for gold nanocrystals.[3,4] Electrochemical studies of redox-modified cluster molecules suggest that they offer promise as multielectron donor/acceptor reagents and catalysts.[5] Conglomeration of these particles by DNA base pairing has been observed and may prove useful in building nanostructures.[6] The thermodynamics of particle formation has been studied and is arguably similar to the more familiar case of a water-in-oil microemulsion.[7]

Alkanethiolate nanocrystals are commonly prepared by a two-phase solution method.[8] $AuCl_4^-$ ions in aqueous solution are reduced to Au^0 leading to gold nucleation into small clusters or nanocrystals. An alkanethiol that is initially dissolved in a nonaqueous phase is vigorously mixed with the gold solution, leading to alkanethiolate adsorption onto the gold nanocrystals. It has been noted that both the length of the alkyl chain and the ratio of alkanethiol to gold influence the size of the nanocrystals.[1,5,9] The sample discussed in this report is the smallest of several stable sizes of nanocrystals produced by octadecanethiol adsorption onto the gold cores. From high-resolution electron microscopy, it is known that the gold cores are compact, faceted, and crystalline.[1] Electron and powder X-ray diffraction experiments have demonstrated that the gold lattice is face-centered cubic.[1,10] The shape of the gold cores has been inferred to be octahedral, decahedral, or icosahedral.[10] These results imply that the core of the nanocrystals is pure gold and that sulfur is present only as linkages to the alkyl chains.

A natural way to determine the size of these particles is by mass spectrometry. Indeed, Whetten and co-workers recorded mass spectra by using laser desorption/ionization coupled with a linear time-of-flight instrument.[1,11] Large nanocrystal ions were observed without the assistance of a matrix, in striking contrast with experimental results on proteins, nucleic acids and synthetic polymers of similar size.[12−15] The smallest stable size of alkanethiolate-coated gold nanocrystals corresponded to a peak at about 15 000 Da with a 2000 Da fwhm. Other peaks appeared at masses of about 23 000 and 29 000 Da. Recent advances in time-of-flight mass spectrometry have enabled significant improvements in the resolution of mass spectra of biopolymers having sizes comparable to these gold nanocrystals.[16] Exploiting these developments, we demonstrate that the previously observed 15 kDa peak actually consists of a series of resolvable peaks and we determine the specific atomic compositions of the corresponding particles.

(1) Whetten, R.; Khoury, J.; Alvarez, M.; Murthy, S.; Vezmar, I.; Wang, Z.; Stephens, P.; Cleveland, C.; Luedtke, W.; Landman, U. *Adv. Mater.* **1996**, *8* (5), 428−433.

(2) See, for example: (a) Bawendi, M.; Steigerwald, M.; Brus, L. *Annu. Rev. Phys. Chem.* **1990**, *41*, 477−496. (b) Henglein, A. *Top. Curr. Chem.* **1988**, *143*, 113. (c) Wang, Y.; Herron, N. *J. Phys. Chem.* **1991**, *95*, 525−532.

(3) Andres, R.; Bein, T.; Dorogi, M.; Feng, S.; Henderson, J.; Kubiak, C.; Mahoney, W.; Osifchin, R.; Reifenberger, R. *Science* **1996**, *272*, 1323−1325.

(4) Terrill, R.; Postlethwaite, T.; Chen, C.; Poon, C.; Terzis, A.; Chen, A.; Hutchison, J.; Clark, M.; Wignall, G.; Londono, J.; Superfine, R.; Falvo, M.; Johnson, C.; Samulski, E.; Murray, R. *J. Am. Chem. Soc.* **1995**, *117*, 12537−12548.

(5) Hostetler, M.; Green, S.; Stokes, J.; Murray, R. *J. Am. Chem. Soc.* **1996**, *118*, 4212−4213.

(6) Mirkin, C.; Letsinger, R.; Mucic, R.; Storhoff, J. *Nature* **1996**, *382*, 607−609.

(7) Leff, D.; Ohara, P.; Heath, J.; Gelbart, W. *J. Phys. Chem.* **1995**, *99*, 7036−7041.

(8) Brust, M.; Walker, M.; Bethell, D.; Schiffrin, D.; Whyman, R. *J. Chem. Soc., Chem. Commun.* **1994**, 801−802.

(9) Alvarez, M.; Khoury, J.; Schaaff, T.; Shafigullin, M.; Vezmar, I.; Whetten, R. *Chem. Phys. Lett.* **1997**, *266*, 1−2, 91−98.

(10) Whetten, R. Personal communication.

(11) Vezmar, I.; Alvarez, M.; Khoury, J.; Salisbury, B.; Shafigullin, M.; Whetten, R. *Z. Phys. D* **1997**, *40*, 147−151.

(12) Karas, M.; Bachmann, D.; Bahr, U.; Hillenkamp, F. *Int. J. Mass. Spectrom. Ion Processes* **1987**, *78*, 53−68.

(13) Karas, M.; Bahr, U.; Giessmann, U. *Mass Spectrom. Rev.* **1997**, *10*, 335−357.

(14) Nordhoff, E.; Kirpekar, F.; Roepstorff, P. *Mass Spectrom. Rev.* **1997**, *15*, 67−138.

(15) Tanaka, K.; Waki, H.; Ido, Y.; Akita, S.; Yoshida, Y.; Yoshida, T. *Rapid Comm. Mass Spectrom.* **1988**, *2*, 151−153.

(16) Colby, S.; King, T.; Reilly, J. *Rapid Commun. Mass Spectrom.* **1994**, *8*, 865−868.

S0002-7863(97)02354-8 CCC: $15.00
Published on Web 01/30/1998

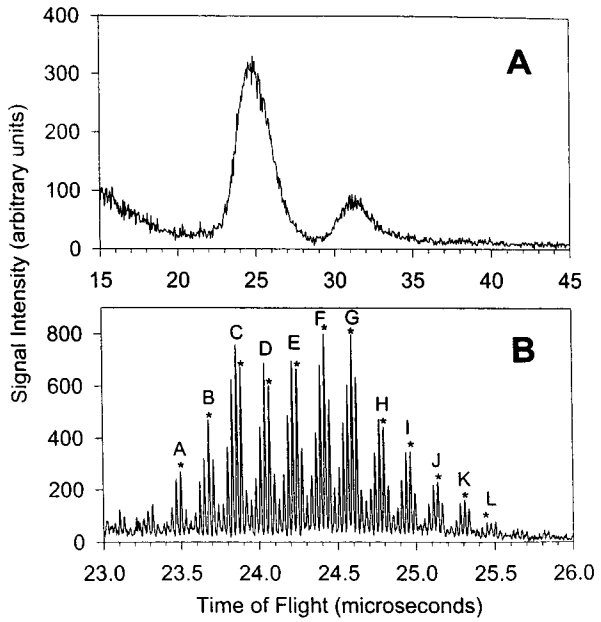

Figure 1. Time-of-flight mass spectra of positive ions produced by 355 nm laser desorption of alkanethiolate-coated gold nanocrystals using (A) DC extraction and (B) pulsed ion extraction. For comparison, MALDI-generated positive ions of cytochrome *c* (12361 Da) and lysozyme (14306 Da) have flight times of 23170.3 and 24924.7 ns, respectively, under the same instrumental conditions as in part B. Peak labels are identified in Table 2.

Procedure

The alkanethiolate-coated gold nanocrystal sample that we studied was obtained from R. Whetten as a solid. The material was dissolved in toluene, using about twice the volume needed to solvate the sample. A small aliquot (generally 1 μL) was then deposited onto the sample probe and the toluene was allowed to evaporate. No matrix was added to this sample spot.

Gold nanocrystal mass spectra were calibrated using cytochrome *c*, ribonuclease A, and lysozyme protein ions obtained by matrix-assisted laser desorption/ionization (MALDI).[10] Ferulic acid and α-cyano-4-hydroxycinnamic acid were the matrixes employed in this part of the work. Our linear time-of-flight instrument was operated using pulsed ion extraction with ion drift energies of 20 keV.[17] Flight tube lengths of 0.335 m for positive ions and 0.231 m for negative ions were used to separate the masses. A few different extraction delays and corresponding drawout voltage pulses were employed. Frequency doubled (532 nm), tripled (355 nm), and quadrupled (266 nm) Nd:YAG laser light and 193 nm ArF excimer laser light were used in these experiments. The YAG harmonics were tightly focused onto the sample using a 30 cm f.l. spherical lens. The excimer laser light was weakly focused to a 1 × 10 mm beam using a cylindrical lens.

Results

A low-resolution mass spectrum of alkanethiolate-coated gold nanocrystal positive ions produced by laser desorption with 355 nm light is shown in Figure 1A. This spectrum is similar to those previously reported by Whetten.[1] A high-resolution expansion of the first peak in this spectrum is displayed in Figure 1B. The center of this distribution of peaks is slightly shifted from the center of the first peak in the low-resolution spectrum because of the voltages used in the pulsed extraction experiment. Masses range from about 12.5 to 15 kDa. The spacings between the clusters labeled with letters correspond to mass shifts of about 197 Da, while spacings within the lettered clusters correspond to mass shifts of about 32 Da. The interpretation immediately suggested is that the lettered clusters have different numbers of gold atoms in the nanocrystal core while the peaks in each cluster correspond to different numbers of sulfur atoms bound to the surface. No peak spacings attributable to $C_{18}H_{37}$ alkyl chains (253.5 Da) are present in the spectrum. For relative comparison, the MALDI-generated positive ions of cytochrome *c* (12 361 Da) and lysozyme (14 306 Da) have flight times of 23 170.3 ns and 24 924.7 ns, respectively, under the same instrumental conditions. A negative ion spectrum, not shown, can also be produced from the same sample and it looks very similar.

While it is readily apparent from the peak separations in Figure 1B that mass spectral features are associated with various numbers of gold and sulfur atoms, establishing the exact number of each is more difficult than one might initially presume. The problem arises from the small difference in mass, 4.583 Daltons, between one gold atom and six sulfur atoms. For example, a certain peak that is tentatively assigned as $Au_{60}S_{36}$ (mass 12 972.324 Da) must be distinguished from $Au_{61}S_{30}$ (mass 12 976.907 Da) or $Au_{59}S_{42}$ (mass 12 967.741 Da). Evidently a convincing assignment of all peaks in the spectrum requires that we establish the mass of each one to an accuracy of about ±1 Da. Mass accuracy of about 0.01% has often been reported in MALDI/time-of-flight mass spectrometry.[18,19] However, those cases involve biomolecular samples using other biopolymers in the same matrix as mass calibration standards. The present situation is somewhat different. When we tried using cytochrome *c* (12 361 Da) and lysozyme (14 306 Da) for mass calibration, the peaks shifted locations by several Daltons depending on the MALDI matrix that we employed. Since the gold alkanethiolate sample was desorbed without any matrix at all, it was not obvious which, if any, matrix should be used in our mass calibration. Our principal concern was that the velocity distributions of laser-desorbed Au_nS_m ions and MALDI-generated ions might differ enough that no matrix would yield accurate mass calibration markers.

To help resolve this problem, we first considered two limiting cases. The peak marked by an asterisk in clump A of Figure 1B was tentatively assigned to a mass of 12 716 on the basis of our rough MALDI mass calibration. Since this is the third peak in clump A, we initially assumed that the smallest number of sulfur atoms that could be associated with it was 2. This, in turn, would imply that 64 Au atoms were present. The maximum number of sulfur atoms that could be bound to the gold core was assumed to correspond to the number of atoms on the surface of a close-packed crystal of 58 gold atoms. This corresponds to about 42 atoms. Thus, the atomic composition of the peaks in clump A of Figure 1B should be between $Au_{64}S_3$ and $Au_{58}S_{40}$. Obviously, we have a better idea about the number of gold atoms in the nanocrystals than about the number of sulfur atoms.

It is well-known that the velocity focusing achieved by pulsed ion extraction is mass dependent and that instrument resolution decreases for masses above and below the one for which conditions have been optimized. As peaks broaden, the accuracy with which masses can be assigned also degrades. However, at the mass for which conditions have been optimized, ion flight time is nearly independent of the velocity with which

(17) Colby, S.; Reilly, J. *Anal. Chem.* **1996**, *68*, 1419−1428.

(18) Beavis, R.; Chait, B. *Anal. Chem.* **1990**, *62*, 1836−1840.

(19) Whittal, R.; Li, L. *Anal. Chem.* **1995**, *67*, 1950−1954.

Table 1. Ribonuclease A and Lysozyme Flight Times: Experiment vs Gold/Sulfur Calibration

	$T = 3\ \mu$s	$T = 4\ \mu$s	$T = 5\ \mu$s	$T = 7\ \mu$s
		Ribonuclease A Flight Times		
MALDI (exp.), ns	25053.52	25218.62	25328.40	25483.13
A = $Au_{60}S_{28}$ (error, Δt)	25054.03 (+0.51)	25220.44 (+1.82)	25329.41 (+1.01)	25484.85 (+1.72)
A = $Au_{61}S_{22}$ (error, Δt)	25049.86 (−3.66)	25216.22 (−2.40)	25325.28 (−3.12)	25480.63 (−2.50)
		Lysozyme Flight Times		
MALDI (exp.), ns	25613.75	25783.73	25895.92	26053.95
A = $Au_{60}S_{28}$ (error, Δt)	25614.88 (+1.13)	25785.19 (+1.46)	25897.08 (+1.16)	26055.91 (+1.96)
A = $Au_{61}S_{22}$ (error, Δt)	25610.80 (−2.95)	25781.00 (−2.73)	25892.92 (−3.00)	26051.72(−2.23)

Table 2. Gold/Sulfur Peak Assignments

cluster	formulae
A	$Au_{60}S_{26,27,28*,29}$
B	$Au_{61}S_{26,27,28*,29}$
C	$Au_{62}S_{26,27,28,29*}$
D	$Au_{63}S_{26,27,28,29*}$
E	$Au_{64}S_{27,28,29*,30}$
F	$Au_{65}S_{27,28,29*,30}$
G	$Au_{66}S_{27,28,29*,30}$
H	$Au_{67}S_{27,28,29,30*}$
I	$Au_{68}S_{28,29,30*,31}$
J	$Au_{69}S_{28,29,30*,31}$
K	$Au_{70}S_{28,29,30*,31}$
L	$Au_{71}S_{29*,30,31}$

an ion is initially desorbed.[17] This situation allows us to use MALDI-generated protein ion masses to calibrate our gold nanocrystal spectrum for peaks that are nearby. Therefore, we set up our mass calibration over the narrow range between ribonuclease A (13 683.2 Da) and lysozyme (14 306 Da). The equation

$$\mathrm{TOF} = (A \times \mathrm{mass}) + (B \times \mathrm{mass}^{1/2}) + \mathrm{C} \qquad (1)$$

provides a fairly accurate calibration for pulsed ion extraction linear TOFMS. Protein masses were used to generate a tentative set of gold nanocrystal peak assignments. Eleven gold nanocrystal flight times and assumed masses were then fit to the equation. Flight times for the known protein ion masses were calculated on the basis of this fit and compared to the experimental values. This process was done using four independent sets of instrument operating conditions. Table 1 lists experimentally measured flight times for ribonuclease A and lysozyme along with their predicted flight times based on two different series of gold formula assignments. For one of these series, the peak marked with an asterisk in clump A of Figure 1B is $Au_{60}S_{28}$; for the other it is $Au_{61}S_{22}$. On the basis of four independent sets of instrument parameters, the former assignment was found to be the optimal one. This led to the formula assignments listed in Table 2 for all of the peaks observed in Figure 1B.

An obvious question that arises is whether the spectrum in Figure 1B provides an accurate representation of the numbers of gold and sulfur atoms in the nanocrystals or whether the ions that we observed were simply fragments of some larger particles. To provide some insight into this issue, we recorded spectra at varying incident laser light pulse energies. These are shown in Figure 2. As the 355 nm light pulse energy increased by over 1 order of magnitude, the spectrum remained essentially unchanged. This result indicates that the observed distribution of gold cluster sizes is in fact representative of the sample and is not drastically altered by laser-induced photodissociation.

Another question that arises is whether the ionization is highly dependent on the incident laser wavelength. The spectra in Figure 3 were obtained by varying the wavelength of laser light used to desorb and ionize the sample. All three wavelengths used, 266, 355, and 532 nm, produced similar spectra.

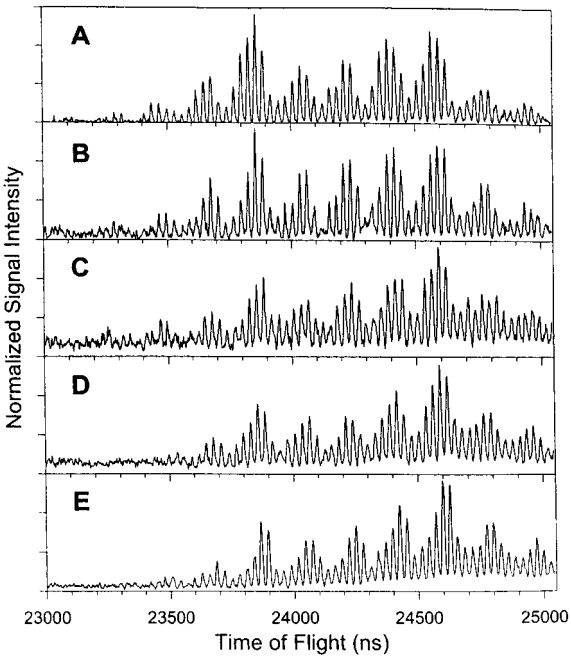

Figure 2. Time-of-flight mass spectra of positive ions produced by 355 nm laser desorption of alkanethiolate-coated gold nanocrystals using (A) 2.7 μJ, (B) 4.7 μJ, (C) 9.0 μJ, (D) 15 μJ, and (E) 27 μJ of light per laser pulse.

Varying the intensity of light used, as done in Figure 2 for 355 nm light, provided some interesting results. As with 355 nm light, changing the 266 nm light pulse energy from about 2.9 to 16.5 μJ per pulse did not dramatically change the spectrum (data not shown). However, changing the 532 nm light pulse energy did have a significant effect as seen in Figure 4. With 64 μJ of 532 nm light per pulse, ions were observed as an unresolved distribution at longer flight time. With 125 or 185 μJ of 532 nm light, well-resolved peaks were observed. The higher light pulse energy required for desorption and ionization with 532 nm light is consistent with the smaller absorption coefficient at the longer wavelength.[9]

The spectrum displayed in Figure 5 shows pure gold cluster ions produced by the two-step process of desorbing the nanocrystals with 355 nm light and then irradiating them 2 ± 0.2 mm above the sample plate with 193 nm light. The numbers of gold atoms in each cluster are marked. Several of the peaks corresponding to 44 or more gold atoms have shoulders, indicating that some sulfur remains attached. However, at smaller cluster sizes, the peaks correspond to pure gold cluster ions. In a high fluence single laser experiment, Vezmar et al.[11] obtained somewhat similar results. We observe approximately 100 times more ions when using both lasers than we see with

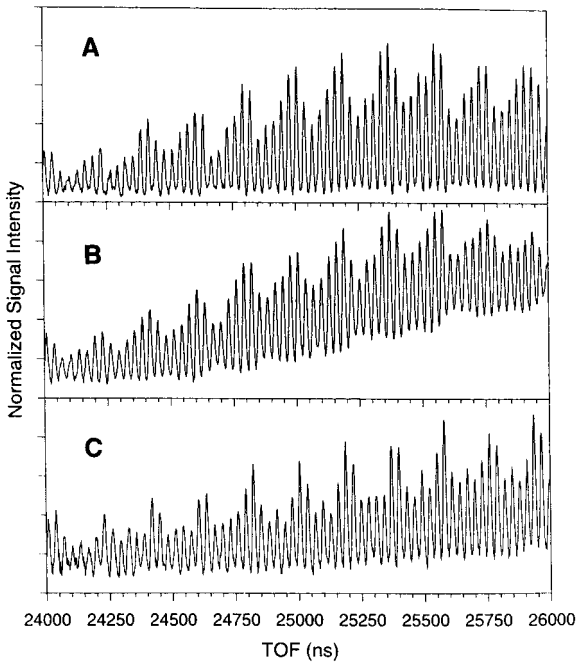

Figure 3. Time-of-flight mass spectra of positive ions produced by laser desorption of alkanethiolate-coated gold nanocrystals using (A) 14 μJ of 266 nm light, (B) 12 μJ of 355 nm light, and (C) 185 μJ of 532 nm light per laser pulse.

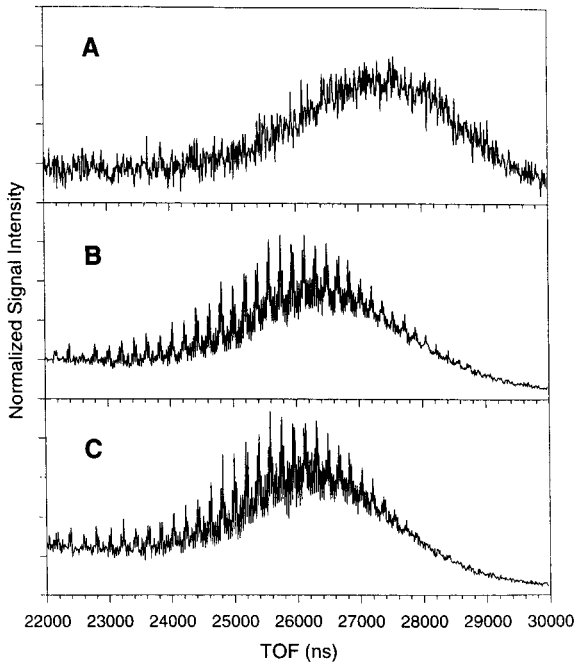

Figure 4. Time-of-flight mass spectra of positive ions produced by 532 nm laser desorption of alkanethiolate-coated gold nanocrystals using (A) 64 μJ, (B) 125 μJ, and (C) 185 μJ of light per laser pulse.

the 355 nm desorption laser alone. This implies that the ArF laser does not simply fragment larger ions but it also photoionizes some clusters. It also indicates that more of the initially desorbed nanocrystals are neutral than are ionized, consistent with the observations of Vezmar et al. The smaller gold cluster ions, containing up to about 40 atoms, display an interesting trend in which the intensities of odd and even number gold cluster ions alternate. This has previously been observed for gold clusters laser ablated from a gold surface and the phenomenon has been attributed to electron pairing in the clusters.[20]

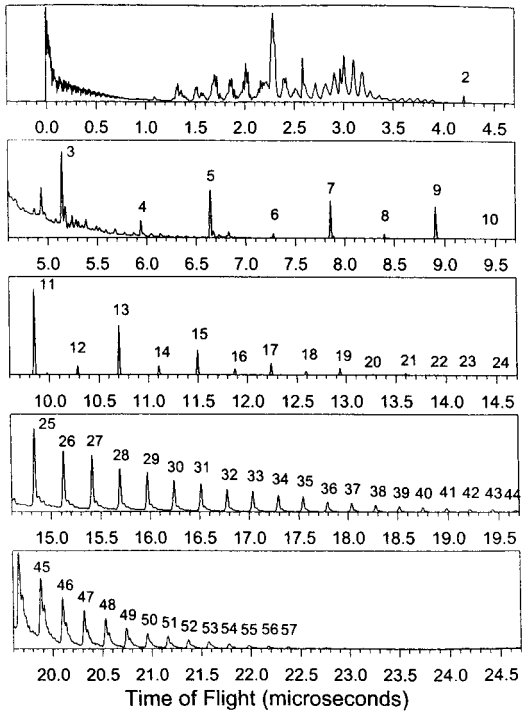

Figure 5. Time-of-flight mass spectrum of positive ions produced by a 355 nm laser pulse ($\sim$10 μJ) applied to the alkanethiolate-coated gold nanocrystal sample followed 4 μs later by a 193 nm laser pulse ($\sim$1.1 mJ) passing 2.0 mm above the sample probe. Ions were pulsed out of the initially field-free source 2 μs after the second laser pulse.

Discussion

No peak spacings in any of the spectra displayed in this paper correspond to the mass of the alkyl chain (253.5 Da) or small hydrocarbon fragments. This implies that the ions detected are composed of only gold and sulfur atoms. To produce ions containing only gold and sulfur, the UV light must selectively and efficiently cleave all the S−C bonds in the nanocrystal. If only some of these bonds were broken in the process, then mass shifts of 253.5 Da would be observed and the spectrum would change dramatically upon varying the light intensity. Yet from Figure 2, it is evident that this is not the case with 355 nm light. Previous experiments on similar alkanethiolate molecules attached to bulk gold have shown that low intensity UV light effectively cleaves the S−C bonds without affecting Au−S linkages.[21] Although this is consistent with our observations, it is in contrast with results of thermal desorption experiments involving alkanethiolate molecules attached to both bulk gold electrodes[22,23] and gold nanoparticles.[4,23,24] In those cases, Au−S bond cleavage was observed. The chemisorption energy of the Au−S interaction has been reported to be approximately 28 kcal/mol (1.2 eV).[7] On the basis of the thermal desorption results, this is apparently the weakest bond in the ground electronic state of the nanocluster. However, following excitation by UV light, repulsion between the S and C atoms apparently develops, leading to dissociation of this bond. The

(20) Katakuse, I.; Ichihara, T.; Fujita, Y.; Matsuo, T.; Sakurai, T.; Matsuda, H. *Int. J. Mass Spectrom. Ion Processes* **1985**, *67*, 229−236.
(21) Lewis, M., Tarlov, M.; Carron, K. *J. Am. Chem. Soc.* **1995**, *117*, 9574−9575.
(22) Delamarche, E.; Michel, B.; Kang, H.; Gerber, C. *Langmuir* **1994**, *10*, 4103−4108.
(23) Schönenberger, C.; Jorritsma, J.; Sondag-Huethorst, J.; Fokkink, L. *J. Phys. Chem.* **1995**, *99*, 3259−3271.
(24) Wingate, J.; Vachet, R.; Hostetler, M.; Murray, R.; Glish, G. 45th ASMS Conference, Palm Springs, CA, June 1−5, 1997.

remarkable selectivity of the fragmentation that we observe is not easily understood or explained. Unfortunately, attempts at theoretically modeling the system are thwarted by the size and complexity of the system.

Figure 4A shows that when a small amount of 532 nm light was used, an unresolved distribution of ions was observed at longer flight time than the well-resolved peaks produced at higher light intensities. Our interpretation is that the unresolved distribution is produced by incomplete cleavage of all the S−C bonds, yielding ions with different numbers of alkyl chains or alkyl fragments attached. Incomplete cleavage is apparently facilitated by the low absorption coefficient at this long wavelength.[9] When enough 532 nm light pulse energy was provided to the sample, the three wavelengths produced similar spectra, as shown in Figure 3.

In an attempt to determine what molecular fragments are desorbed from the gold core, we looked at the positive ions in the low mass (less than 400 Da) region of the spectrum. With the exception of a single peak at $m/z = 197$ that probably corresponds to Au^+, all fragment ions in this mass region could be associated with hydrocarbon fragments containing from two to nine carbon atoms. The 197 Da peak represents about 2% of the total intensity of the ions between 10 and 400 Da. No evidence of any sulfur-containing ions and no larger clusters of gold (Au_n^+) were found. These observations indicate that most of the material removed from the gold core during laser desorption of the alkanethiolate-coated nanocrystals is hydrocarbon without sulfur or gold.

The two-laser experiment shows that many more neutral molecules than ions were produced by the 355 nm desorption laser. The energy of 355 nm photons is 3.49 eV, which is less than the 5.1 eV work function of bulk gold. This light seems to be able to efficiently break the S−C bonds of the alkanethiolate chains by radical cleavage and thereby desorb the gold cores with many sulfur atoms attached. The second laser (193 nm) provides 6.43 eV per photon, easily more than the work function of bulk gold, allowing for more efficient ionization along with fragmentation of the desorbed gold cores. This ionization with the second laser probably occurs by photoemission as from bulk metal surfaces. With the two-laser experiment, we demonstrate, through choice of laser wavelength and intensity, some control over the very selective type of fragmentation that occurs with these nanocrystals.

While the present work has focused on the interpretation and identification of ion peaks in a mass spectrum, from a more global perspective our goal is to understand the composition of the alkanethiolate-coated gold nanocrystals that were originally deposited onto the sample probe. Preceding irradiation by the desorption laser, $C_{18}H_{37}$ alkyl groups are bonded to all S atoms on the surfaces of the gold particles. On the basis of our experiments varying the 355 nm light intensity and also from looking at the low-mass region of the spectrum, we infer that the numbers of sulfur and gold atoms in the observed ions are not dramatically different than in the original sample. Thus, these experiments allow us to ascertain the composition of the alkanethiolate-coated gold nanocrystals within the mass range investigated.

Conclusions

We have shown that alkanethiolate-coated gold nanocrystals can be laser desorbed and ionized without the assistance of a matrix and mass analyzed with good resolution by pulsed ion extraction. We have assigned masses and formulas to the observed ions, thereby deriving precise information about the compositions of the ions. Laser irradiation of the sample efficiently cleaves the S−C bonds in the alkanethiolate chain, so that the ions detected are composed of only gold and sulfur atoms. The observed ratio of sulfur to gold atoms suggests that most of the surface sites on the gold core are occupied by sulfur atoms. We have no evidence to suggest that the numbers of gold and sulfur atoms in the nanocrystals are significantly changed by the desorption process. More experiments beyond those discussed here will be required to confirm this mechanism of fragmentation. In a two-laser experiment, we have shown that various sizes of pure gold cluster ions can be generated from the large number of neutral particles that are initially desorbed from the alkanethiolate-coated gold nanocrystal sample.

Alkanethiolate-coated gold nanocrystals are under investigation in a range of disciplines, including physics, materials science, and electrochemistry. Information about the exact composition of these molecules as described in this report may lead to improved understanding of their properties and to possible new applications.

Acknowledgment. The authors wish to thank Professor R. Whetten for providing the sample of alkanethiolate coated gold nanocrystals investigated in this study. Support for this work was provided by the National Science Foundation.

JA9723545